Article

Cell Reports

IL-15 enhances CCR5-mediated migration of memory CD8$^+$ T cells by upregulating CCR5 expression in the absence of TCR stimulation

Graphical abstract

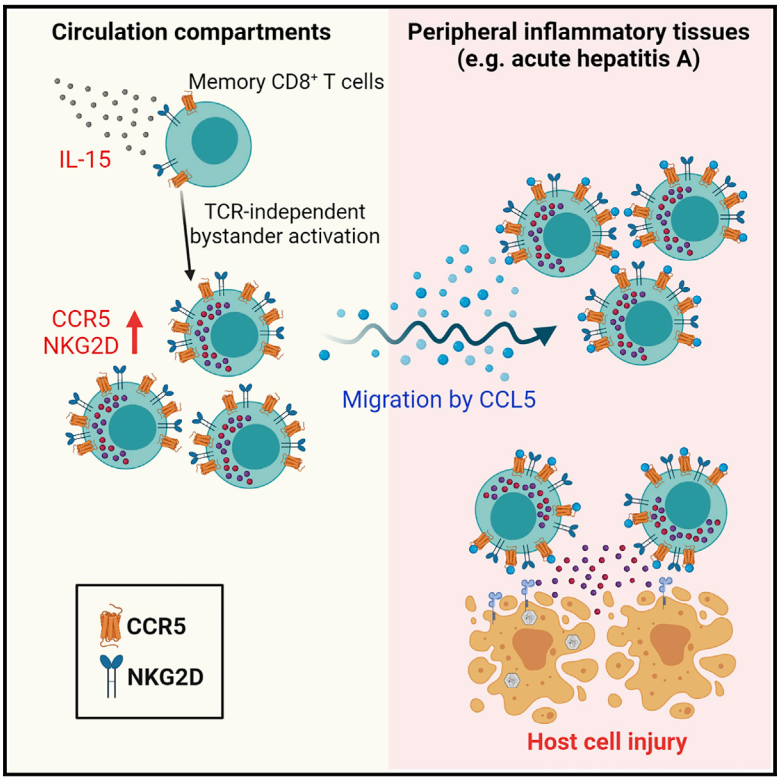

Highlights

- IL-15 upregulates CCR5 in memory CD8$^+$ T cells in the absence of TCR stimulation
- CCR5 is upregulated in IL-15-induced bystander-activated CD8$^+$ T cells
- IL-15-treated CD8$^+$ T cells migrate in a CCR5-dependent manner
- CCR5 upregulation is associated with liver injury during acute hepatitis A

Authors

In-Ho Seo, Hyuk Soo Eun, Ja Kyung Kim, ..., Won Kim, Su-Hyung Park, Eui-Cheol Shin

Correspondence

drwon1@snu.ac.kr (W.K.), park3@kaist.ac.kr (S.-H.P.), ecshin@kaist.ac.kr (E.-C.S.)

In brief

IL-15 induces TCR-independent bystander activation of memory CD8$^+$ T cells. Seo et al. demonstrate that IL-15 upregulates CCR5 expression on memory CD8$^+$ T cells and enhances CCR5-mediated migration. During acute hepatitis A, CCR5 is upregulated in bystander-activated CD8$^+$ T cells and associated with liver injury.

Seo et al., 2021, Cell Reports *36*, 109438
July 27, 2021
https://doi.org/10.1016/j.celrep.2021.109438

CellPress

Cell Reports

CellPress
OPEN ACCESS

Article

IL-15 enhances CCR5-mediated migration of memory CD8$^+$ T cells by upregulating CCR5 expression in the absence of TCR stimulation

In-Ho Seo,[1,5] Hyuk Soo Eun,[2,5] Ja Kyung Kim,[3,5] Hoyoung Lee,[1] Seongju Jeong,[1] Seong Jin Choi,[1] Jeewon Lee,[1] Byung Seok Lee,[2] Seok Hyun Kim,[2] Woo Sun Rou,[2] Dong Hyeon Lee,[4] Won Kim,[4,*] Su-Hyung Park,[1,*] and Eui-Cheol Shin[1,5,6,*]

[1]Graduate School of Medical Science and Engineering, Korea Advanced Institute of Science and Technology, Daejeon 34141, Republic of Korea
[2]Department of Internal Medicine, Chungnam National University School of Medicine, Daejeon 35015, Republic of Korea
[3]Department of Internal Medicine, Yongin Severance Hospital, Yonsei University College of Medicine, Yongin 16995, Republic of Korea
[4]Department of Internal Medicine, Seoul Metropolitan Government Seoul National University Boramae Medical Center, Seoul National University College of Medicine, Seoul 07061, Republic of Korea
[5]These authors contributed equally
[6]Lead contact
*Correspondence: drwon1@snu.ac.kr (W.K.), park3@kaist.ac.kr (S.-H.P.), ecshin@kaist.ac.kr (E.-C.S.)
https://doi.org/10.1016/j.celrep.2021.109438

SUMMARY

During microbial infection, bystander CD8$^+$ T cells that are not specific to infecting pathogens can be activated by interleukin (IL)-15. However, the tissue-homing properties of bystander-activated CD8$^+$ T cells have not been elucidated. Here, we examine the effects of IL-15 on the expression of chemokine receptors on CD8$^+$ T cells and their migration. IL-15 upregulates CCR5 in memory CD8$^+$ T cells in the absence of T cell receptor (TCR) stimulation and enhances CCR5-dependent migration. IL-15-induced CCR5 upregulation is abrogated by TCR stimulation, indicating that CCR5 is upregulated in bystander-activated CD8$^+$ T cells. Moreover, CCR5 signals increase proliferation and cytotoxic protein expression in IL-15-treated memory CD8$^+$ T cells, although the increase has a small extent. CCR5 upregulation in bystander-activated CD8$^+$ T cells is associated with severe liver injury in patients with acute hepatitis A. Altogether, the results indicate that CCR5 upregulation by IL-15 mediates the migration of bystander-activated CD8$^+$ T cells.

INTRODUCTION

During microbial infection, CD8$^+$ T cells specific to the infecting pathogen are activated by T cell receptors (TCRs) that recognize the epitope peptides presented by major histocompatibility complex class I (MHC class I) molecules. Following activation, the CD8$^+$ T cells exert effector functions, including cytotoxicity and cytokine production, contributing to the elimination of pathogenic microbes (Wong and Pamer, 2003).

Bystander CD8$^+$ T cells that are specific to antigens other than the infecting pathogens can also be activated by antigen-independent mechanisms during certain microbial infections (Kim and Shin, 2019; Tough et al., 1996; Whiteside et al., 2018). In a murine model, memory CD8$^+$ T cells primed by vesicular stomatitis virus infection were found to be activated by subsequent *Listeria* infection (Chu et al., 2013). Similarly, memory CD8$^+$ T cells primed by lymphocytic choriomeningitis virus or *Listeria* were activated following *Leishmania* infection (Crosby et al., 2014). In humans, activation of bystander CD8$^+$ T cells has been demonstrated in patients infected with hepatitis A virus (HAV) (Kim et al., 2018), hepatitis B virus (Sandalova et al., 2010), hepatitis C virus (Alanio et al., 2015), human immunodeficiency virus (Bastidas et al., 2014; Doisne et al., 2004; Younes et al., 2016), or hantavirus (Tuuminen et al., 2007). In patients with acute HAV infection, preexisting memory CD8$^+$ T cells that are specific to common viruses, but not HAV, are activated by interleukin (IL)-15 that is over-produced in HAV infection (Kim et al., 2018).

Bystander-activated CD8$^+$ T cells can play a beneficial or detrimental role in hosts during infection. For example, in a model of *Listeria* infection, bystander-activated CD8$^+$ T cells contribute to the early control of pathogens (Chu et al., 2013), whereas bystander-activated CD8$^+$ T cells promote immune-mediated host injury in a model of *Leishmania* infection (Crosby et al., 2014). In patients with acute HAV infection, the activation of bystander CD8$^+$ T cells is associated with severe liver injury (Kim et al., 2018). In this process, bystander CD8$^+$ T cells are activated by IL-15 (Kim et al., 2018; Liu et al., 2002; Soudja et al., 2012) and acquire cytolytic activity mediated by natural killer (NK)-activating receptors, such as NKG2D and NKp30, without TCR stimulation (Kim et al., 2018, 2020). Intriguingly, the expression of NKG2D on the cell surface of memory CD8$^+$ T cells is upregulated by IL-15 only when TCR stimulation with

cognate antigens is absent (Kim et al., 2018); thus, the upregulation of NKG2D on memory CD8$^+$ T cells is an indicator of IL-15-induced activation in the absence of TCR stimulation.

Although the roles of bystander-activated CD8$^+$ T cells and related mechanisms have been studied as described earlier, their tissue-homing properties have not been investigated. More specifically, which chemokine receptors are upregulated by IL-15 in the absence of TCR stimulation in memory CD8$^+$ T cells has not been studied. In addition, whether chemokine receptors upregulated by IL-15 play a role in the migration of bystander-activated CD8$^+$ T cells to the site of microbial infection is not clear.

In the present study, we examined how IL-15 changes the expression of chemokine receptors in memory CD8$^+$ T cells in the absence of TCR stimulation. We also examined whether IL-15-induced chemokine receptors regulate the migration of bystander-activated memory CD8$^+$ T cells. Finally, we investigated a possible role of IL-15-induced chemokine receptors on bystander-activated CD8$^+$ T cells in severe liver injury in patients with acute HAV infection.

RESULTS

IL-15 induces CCR5 upregulation in memory CD8$^+$ T cells without TCR stimulation

In the present study, we focused on CCR7$^-$CD45RA$^-$ effector memory T (T_{EM}) and CCR7$^-$CD45RA$^+$ effector memory T (T_{EMRA}) cells; thus, we sorted or gated CCR7$^-$ memory CD8$^+$ T cells to investigate the effect of IL-15. First, we examined which chemokine receptors are modulated by IL-15 in human memory CD8$^+$ T cells in the absence of TCR stimulation. We sorted CCR7$^-$ memory CD8$^+$ T cells from four healthy donors and cultured them for 48 h with or without IL-15 treatment before performing RNA sequencing (RNA-seq) analysis. Among chemokine receptors, CCR5 expression was significantly increased by IL-15 (Figure 1A). Therefore, we focused on CCR5 in subsequent experiments.

Next, we incubated peripheral blood mononuclear cells (PBMCs) from healthy donors with IL-15 and/or anti-CD3 stimulation and examined CCR5 expression. IL-15 increased the percentage of CCR5$^+$ cells among CCR7$^-$ memory CD8$^+$ T cells, whereas anti-CD3 decreased it (Figure 1B). Anti-CD3 abrogated IL-15-induced upregulation of CCR5, indicating that IL-15 increases CCR5 expression in bystander-activated memory CD8$^+$ T cells in the absence of TCR activation. We also examined the effects of IL-15 and/or cytomegalovirus (CMV) $pp65_{495}$ peptide (NLVPMVATV) on the frequency of CCR5$^+$ cells among HLA-A*02 CMV $pp65_{495}$ multimer$^+$ cells. IL-15 increased the percentage of CCR5$^+$ cells, whereas NLVPMVATV peptide decreased it (Figure 1C). In addition, NLVPMVATV peptide significantly decreased IL-15-induced CCR5 upregulation, similar to anti-CD3. These data are reminiscent of our previous results showing that IL-15 increases NKG2D expression on memory CD8$^+$ T cells only in the absence of TCR stimulation (Kim et al., 2018). We also performed CCR5 staining following cell permeabilization to stain total CCR5, including cell surface and intracellular CCR5. We found that IL-15 stimulation increased the expression of total CCR5, as well as the expression of cell surface CCR5 (Figure S1A). We confirmed IL-15-induced upregulation of CCR5 in sorted CCR7$^-$ memory CD8$^+$ T cells (Figure 1D).

We examined the effects of other common γ chain cytokines in PBMC cultures. IL-2 and IL-7 did not increase the percentage of CCR5$^+$ cells among memory CD8$^+$ T cells (Figure 1E). We found that the expression of other chemokine receptors, including CX3CR1, CXCR3, and CCR2, was not upregulated by common γ chain cytokine or anti-CD3 stimulation (Figure S1B). We also examined the effect of IL-15 on the expression of chemokine receptors separately in CCR7$^-$CD45RA$^-$ T_{EM} and CCR7$^-$CD45RA$^+$ T_{EMRA} cells and found that IL-15 upregulated the expression of CCR5 in both T cell populations, but not the expression of other chemokine receptors (Figure S1C). This effect of IL-15 on CCR5 expression was not observed in CD4$^+$CD25$^+$FoxP3$^+$ regulatory T (Treg) cells (Figure 1F), non-Treg CCR7$^-$ memory CD4$^+$ T cells (Figure 1G), or TCR Vα7.2$^+$CD161$^+$ mucosal-associated invariant T (MAIT) cells (Figure S1D). Altogether, these data demonstrate that IL-15-induced, TCR-independent activation of memory CD8$^+$ T cells results in upregulation of CCR5.

IL-15-treated memory CD8$^+$ T cells migrate in a CCR5-dependent manner

We assessed the migration ability of IL-15-treated memory CD8$^+$ T cells using transwell migration assays (Figure 2A). CCR7$^-$ memory CD8$^+$ T cells were sorted from PBMCs obtained from healthy donors and incubated with or without IL-15 for 48 h. Those cells were placed on the upper inserts in transwell systems and CCL5 in the lower chambers and incubated for 3 h. CCL5-induced migration was significantly higher in IL-15-treated memory CD8$^+$ T cells than in non-treated controls (Figure 2B).

Next, we investigated the effect of IL-15 on memory CD8$^+$ T cells in mice. We adoptively transferred CD45.1$^+$OT-1 CD8$^+$ T cells into B6 mice and primed them with vaccinia virus-expressing ovalbumin (VV-OVA). After resolution of VV-OVA infection, we sorted memory OT-1 CD8$^+$ T cells using the CD45.1 congenic marker. When we treated the cells with IL-15 *in vitro*, the percentage of CCR5$^+$ cells significantly increased, but the percentage of CCR2$^+$ or CXCR3$^+$ cells did not (Figure 2C). We also examined the effects of IL-15 in the presence of SIINFEKL peptide. IL-15 increased the percentage of CCR5$^+$ cells among memory OT-1 T cells, whereas SIINFEKL peptide decreased it (Figure 2D). In addition, SIINFEKL peptide significantly decreased IL-15-induced CCR5 upregulation.

For *in vivo* migration assays, sorted memory CD45.1$^+$OT-1 T cells were treated with or without IL-15 and adoptively transferred to naive B6 mice. Maraviroc, a CCR5 antagonist, was used with IL-15 to block the effect of CCR5. The mice were infected with PR8 influenza virus and sacrificed, and then we quantified the CD45.1$^+$OT-1 T cells that migrated to the lung tissues (Figure S2). IL-15-treated CD45.1$^+$OT-1 T cells were abundant in PR8-infected lung tissues, whereas non-treated CD45.1$^+$OT-1 T cells were scarce (Figure 2E). Importantly, the migration of IL-15-treated CD45.1$^+$OT-1 T cells was significantly reduced by maraviroc treatment, indicating that the migration of IL-15-treated OT-1 cells was mediated by CCR5. We also examined the expression of Ki-67, a marker of cell proliferation, in CD45.1$^+$OT-1 T cells harvested from lung tissue and found that almost all IL-15-treated CD45.1$^+$OT-1 T cells expressed Ki-67, whereas non-treated CD45.1$^+$OT-1 T cells hardly expressed Ki-67 (Figure 2F). Maraviroc treatment significantly decreased

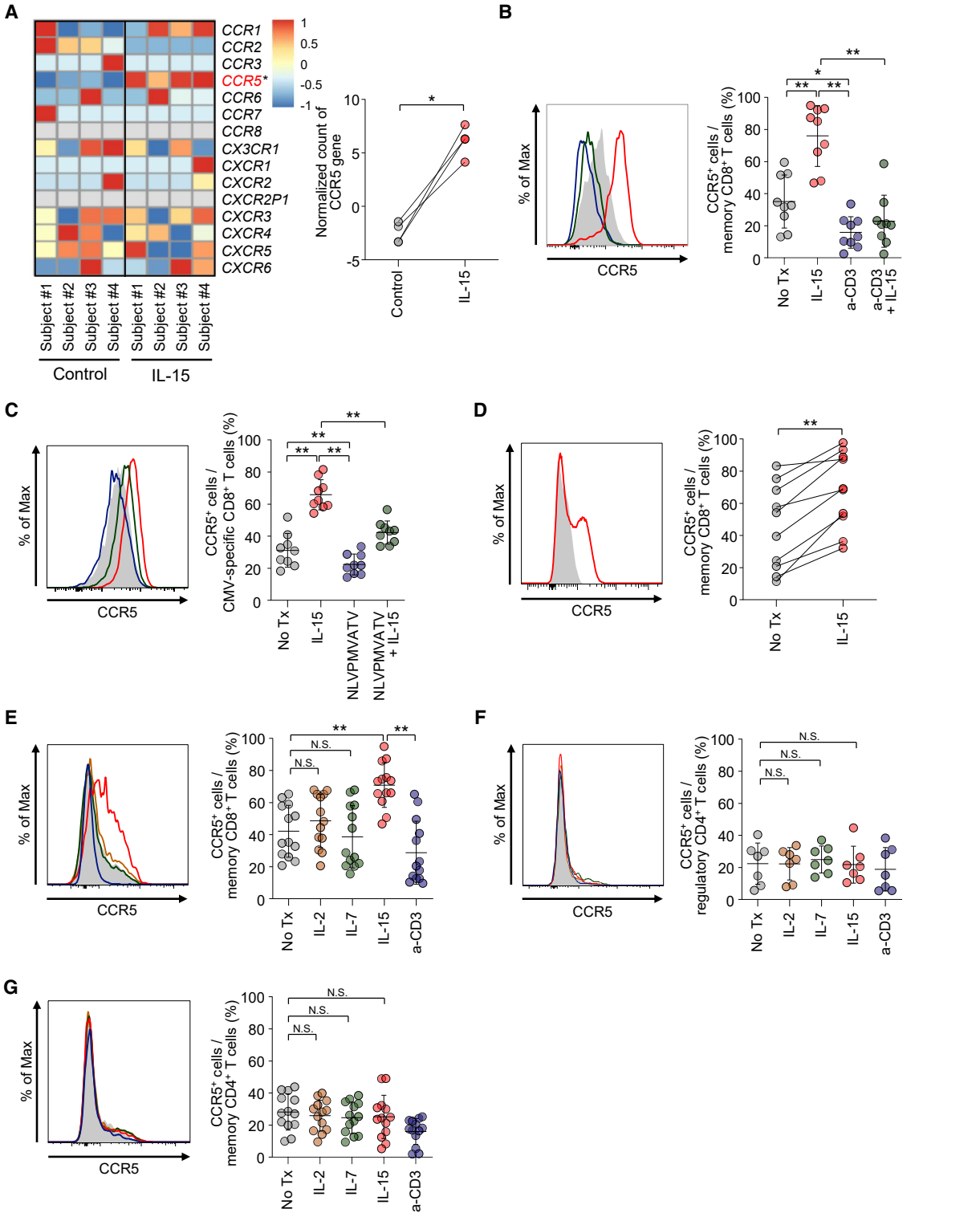

Figure 1. IL-15 induces CCR5 upregulation in memory CD8$^+$ T cells without TCR stimulation

(A) CCR7$^-$CD8$^+$ T cells sorted from the PBMCs of healthy donors (n = 4) were cultured with or without IL-15 (10 ng/mL) and analyzed by RNA sequencing. Left, heatmap showing the expression of chemokine receptor genes in control and IL-15-stimulated CCR7$^-$CD8$^+$ T cells. Right, expression of CCR5 in control and IL-15-stimulated CCR7$^-$CD8$^+$ T cells.

(legend continued on next page)

the percentage of Ki-67$^+$ cells in migrated CD45.1$^+$OT-1 T cells, although the decrease had a small extent, indicating that CCR5 is involved in not only the migration of IL-15-treated memory CD8$^+$ T cells but also their proliferation.

CCR5 signals upregulate proliferation and cytotoxic proteins in memory CD8$^+$ T cells in combination with IL-15 via the ERK pathway

Because we found evidence that CCR5 upregulation by IL-15 plays a role in the proliferation of memory CD8$^+$ T cells (Figure 2F), we examined the direct effect of CCL5, a CCR5 ligand, on memory CD8$^+$ T cells following IL-15 treatment (Figure S3A). Although CCL5 treatment without IL-15 pretreatment did not increase Ki-67 expression, CCL5 significantly enhanced Ki-67 upregulation in CCR7$^-$ memory CD8$^+$ T cells pretreated with IL-15 (Figure 3A; Figure S3B). Moreover, CCL5 significantly enhanced the expression of perforin and granulysin in CCR7$^-$ memory CD8$^+$ T cells pretreated with IL-15 even though the increase had a small extent, whereas CCL5 treatment without IL-15 pretreatment did not increase expression of perforin and granulysin. The expression of granzyme B was not enhanced by CCL5 but was significantly increased by IL-15. However, these effects of CCL5 were not observed when we used CCL3 or CCL4 as a ligand for CCR5 (Figure S3C), indicating that among CCR5 ligands, CCL5 plays a specific role in enhancing IL-15-induced memory CD8$^+$ T cell activation. In cell proliferation assays, we confirmed that CCL5 significantly enhances the proliferation of IL-15-treated CCR7$^-$ memory CD8$^+$ T cells (Figure 3B).

We examined which signaling pathway contributes to the effect of CCL5/CCR5 on IL-15-treated CCR7$^-$ memory CD8$^+$ T cells by repeating the CCL5 and IL-15 treatment in the presence of PD98059, an inhibitor of the extracellular signal-regulated kinase (ERK) pathway (Figure S3D). We found that the enhanced expression of Ki-67 by CCL5 in IL-15-pretreated CCR7$^-$ memory CD8$^+$ T cells was abolished by PD98059 (Figure 3C). Similar results were observed when the expression of perforin and granulysin was examined. Altogether, the results indicate that CCL5-CCR5 signals contribute not only to the migration of memory CD8$^+$ T cells activated by IL-15 but also to their enhanced proliferation and cytotoxic capacity.

CCR5 is upregulated on memory CD8$^+$ T cells and correlates with inflammation in patients with acute hepatitis A

Finally, we examined the expression of CCR5 on CCR7$^-$ memory CD8$^+$ T cells in patients with acute hepatitis A (AHA) caused by HAV infection. Previously, our group demonstrated that HAV-unrelated bystander memory CD8$^+$ T cells are activated by IL-15 without TCR stimulation and that bystander-activated CD8$^+$ T cells contribute to liver injury during AHA (Kim et al., 2018). In the present study, we found that the percentage of CCR5$^+$ cells among total CCR7$^-$ memory CD8$^+$ T cells was significantly increased in the peripheral blood of patients with AHA compared with healthy donors (Figure 4A). The increased percentage of CCR5$^+$ cells in the acute stage was reduced when patients were convalescent (Figure 4B). The percentage of CCR5$^+$ cells among CD8$^+$ T cells specific to CMV, an unrelated virus, was significantly higher than the percentage among CD8$^+$ T cells specific to HAV, the infecting virus, in the peripheral blood of patients with AHA (Figure 4C), confirming CCR5 upregulation in bystander-activated CD8$^+$ T cells. We also examined CCR5 expression on CMV-specific CD8$^+$ T cells from healthy donors and found that the frequency of CCR5$^+$ cells was significantly higher in patients with AHA than in healthy donors, indicating that acute HAV infection increases the expression of CCR5 on CMV-specific CD8$^+$ T cells.

We examined whether CD8$^+$ T cells obtained from the peripheral blood of patients with AHA have the ability to migrate in response to CCL5. In transwell migration assays, CD8$^+$ T cells from patients with AHA more efficiently migrated in response to CCL5 than those from healthy donors (Figure 4D). Because CCL5 was previously shown to be produced by HAV-infected cells (Sung et al., 2017), we examined whether CCR5$^+$ cells are more enriched among liver-infiltrating CD8$^+$ T cells than peripheral blood CD8$^+$ T cells. The percentage of CCR5$^+$ cells among liver-infiltrating CD8$^+$ T cells was significantly higher than the percentage among peripheral blood CD8$^+$ T cells in patients with AHA (Figure 4E). We also found that the percentage of CCR5$^+$ cells among peripheral blood CD8$^+$ T cells significantly correlated with serum alanine aminotransferase (ALT), a marker of liver injury (Figure 4F). This suggests that CCR5$^+$CD8$^+$ T cells may be involved in liver injury, which is mediated by IL-15-induced bystander-activated CD8$^+$ T cells, during AHA.

DISCUSSION

Bystander-activated CD8$^+$ T cells play a beneficial or detrimental role to hosts during microbial infection (Chu et al., 2013; Crosby et al., 2014; Kim et al., 2018), but how these cells migrate to sites of inflammation is unclear. Here, we showed that IL-15 upregulated CCR5 in memory CD8$^+$ T cells in the absence of TCR stimulation and enhanced CCR5-dependent migration *in vitro* and *in vivo*. We also found that CCR5 signals increased the proliferation

(B) PBMCs from healthy donors (n = 9) were stimulated with IL-15 (10 ng/mL), anti-CD3 antibody (100 ng/mL), or both for 48 h and analyzed by flow cytometry. The frequency of CCR5$^+$ cells among CCR7$^-$CD8$^+$ T cells was examined, and a representative fluorescence-activated cell sorting (FACS) plot (left) and summary data (right) are presented.
(C) PBMCs from healthy donors (n = 9) were stimulated with IL-15 (10 ng/mL), CMV pp65$_{495}$ peptide (NLVPMVATV) (1 μg/mL), or both for 48 h and analyzed by flow cytometry. The frequency of CCR5$^+$ cells among HLA-A*02 CMV pp65$_{495}$ multimer$^+$ cells was examined, and a representative FACS plot (left) and summary data (right) are presented.
(D) Sorted CCR7$^-$CD8$^+$ T cells from healthy donors (n = 10) were cultured with or without IL-15 (10 ng/mL) for 48 h. The frequency of CCR5$^+$ cells among CCR7$^-$CD8$^+$ T cells was analyzed, and a representative FACS plot (left) and summary data (right) are presented.
(E–G) PBMCs from healthy donors were stimulated with IL-2 (10 ng/mL), IL-7 (10 ng/mL), IL-15 (10 ng/mL), or anti-CD3 antibody (100 ng/mL) for 48 h. The frequency of CCR5$^+$ cells among CCR7$^-$CD8$^+$ T cells (E, n = 13), regulatory CD4$^+$ T cells (F, n = 7), and CCR7$^-$CD4$^+$ T cells (G, n = 13) was analyzed by flow cytometry. Representative FACS plots (left) and summary data (right) are presented.
Data are presented as mean and SD. N.S., not significant; *p < 0.05, **p < 0.01; Wilcoxon matched-pairs signed-rank test.

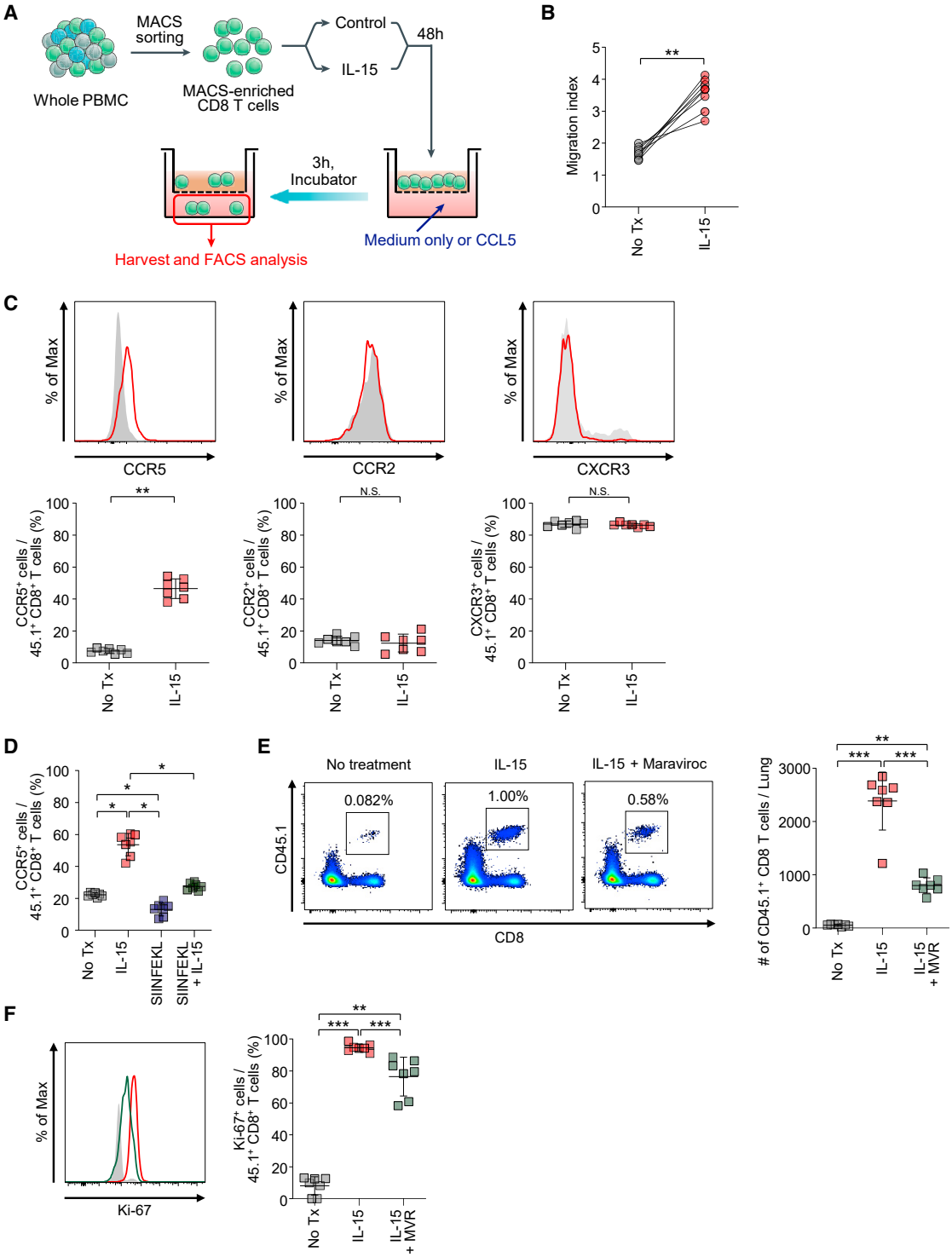

Figure 2. IL-15-treated memory CD8$^+$ T cells migrate in a CCR5-dependent manner *in vitro* and *in vivo*

(A and B) Sorted CCR7$^-$CD8$^+$ T cells from the PBMCs of healthy donors (n = 8) were cultured with or without IL-15 (10 ng/mL) for 48 h, transferred to a transwell culture system, and then incubated at 37°C for 3 h. The migration index was obtained by calculating the number of CCR7$^-$CD8$^+$ T cells that migrated to the lower chamber containing CCL5. (A) Schematic showing the experimental scheme for transwell migration assays. (B) Summary data showing the migration index of control or IL-15-stimulated CCR7$^-$CD8$^+$ T cells.

(legend continued on next page)

and expression of cytotoxic proteins, including perforin and granulysin, in IL-15-treated memory CD8$^+$ T cells. Importantly, IL-15-induced CCR5 upregulation was abrogated by concurrent TCR stimulation. Because IL-15 production is increased during acute viral infection, it is highly likely that bystander-activated CD8$^+$ T cells upregulate CCR5 expression and migrate to sites of inflammation in a CCR5-dependent manner.

IL-15 can activate memory CD8$^+$ T cells in the absence of TCR stimulation (Kim et al., 2020; Liu et al., 2002; Soudja et al., 2012) and induce the innate-like cytotoxic activity of bystander-activated CD8$^+$ T cells (Kim et al., 2018). In addition, we recently reported that IL-15 induces an activation of mucosal-associated invariant T cells to exert innate-like cytotoxic activity in the absence of TCR stimulation (Rha et al., 2020). However, the effect of IL-15 on the expression of chemokine receptors in bystander-activated CD8$^+$ T cells has not been clearly elucidated. A previous study examined the effects of IL-15 on the mRNA expression of chemokines and chemokine receptors in human CD3$^+$ T cells (Perera et al., 1999). It reported that IL-15 upregulated CCL3, CCL4, and CCL5 among chemokines and CCR1, CCR4, and CCR5 among chemokine receptors. In the current study, we focused on CCR7$^-$ memory CD8$^+$ T cells, not total CD3$^+$ T cells, and found that CCR5 is significantly upregulated by IL-15 at not only the mRNA level but also the cell surface protein level. IL-15-induced CCR5 upregulation was more prominent in the culture of PBMCs (Figure 1B) than in the culture of sorted memory CD8$^+$ T cells (Figure 1D). In the PBMC culture, IL-15 could influence memory CD8$^+$ T cells not only directly but also indirectly via effects on other immune cells. However, only direct effects could be examined in the culture of sorted memory CD8$^+$ T cells.

In the current study, IL-15 upregulated the expression of CCR5 in memory CD8$^+$ T cells, but not Treg cells and memory CD4$^+$ T cells (Figures 1F and 1G). In general, IL-15 has potent activity in NK cells and CD8$^+$ T cells compared with CD4$^+$ T cells in terms of cellular proliferation and cytotoxicity (Judge et al., 2002; Lu et al., 2002). Previously, IL-15 was shown to upregulate the expression of cytotoxic proteins such as perforin and granzymes and NK receptors such as NKG2D and NKp30 (Kim et al., 2018). However, such effects were not reported in CD4$^+$ T cells. The relative hyporesponsiveness of CD4$^+$ T cells to IL-15 may not be limited to the expression of CCR5 but may also be observed in the expression of other molecules, including cytotoxic proteins and NK receptors.

We found that CCR5 expression was upregulated by IL-15, but not by anti-CD3 stimulation. Interestingly, CCR5 expression was not upregulated by IL-15 in the presence of anti-CD3. These data indicate that IL-15-induced CCR5 upregulation occurs more selectively among bystander-activated CD8$^+$ T cells that do not have TCR-mediated signals. We suggest that upregulated CCR5 expression on circulating memory CD8$^+$ T cells can be considered a marker of IL-15-induced bystander activation rather than TCR-driven activation. We previously observed similar results in IL-15-induced NKG2D upregulation (Kim et al., 2018). In the previous study, we showed that IL-15 upregulated NKG2D expression on memory CD8$^+$ T cells only in the absence of TCR stimulation. Based on these data, we successfully distinguished bystander-activated CD8$^+$ T cells from cognate antigen-stimulated CD8$^+$ T cells by examining cell surface levels of NKG2D. In that study, TCR abrogated IL-15-induced NKG2D upregulation partly by calpain activity and Jak1 downregulation. Whether IL-15-induced CCR5 upregulation is regulated in similar ways needs to be investigated.

CXCR3 was reported to be an important chemokine receptor for the activation of bystander T cells (Maurice et al., 2019). In this previous study, memory CD8$^+$ T cells were recruited to the site of bystander activation, where T cells clustered around antigen-presenting cells in a CXCR3-dependent manner and underwent bystander activation. Although the role of chemokine receptors was examined in the context of bystander activation, this previous study and our current study have different views. The previous study highlighted CXCR3 as a chemokine receptor for the migration of memory CD8$^+$ T cells to the site of bystander activation. In contrast, our study examined CCR5 as a chemokine receptor for the migration of IL-15-induced bystander-activated CD8$^+$ T cells to the site of infection or inflammation. During microbial infections that result in systemic upregulation of IL-15, bystander memory CD8$^+$ T cells may be activated by IL-15 not only at the site of infection but also systemically. In this situation, CCR5 ligands that are over-produced at the site of infection may recruit CCR5-upregulated bystander-activated CD8$^+$ T cells to the site of infection. Recruited bystander-activated CD8$^+$ T cells can then exert innate-like cytotoxic activity and contribute to host tissue injury. IL-15-induced CCR5 upregulation can also contribute to the retention of CD8$^+$ T cells in inflammatory sites until the resolution of inflammation. Whether IL-15-induced CCR5 upregulation is involved in the maintenance of tissue-resident memory CD8$^+$ T cells needs to be investigated further.

In the current study, we found that CCL5 treatment increases the proliferation and expression of cytotoxic proteins, such as perforin and granulysin, in memory CD8$^+$ T cells when combined with IL-15, even though the increase had a small extent. We also found that these effects of CCL5 are mediated by ERK signaling pathways. Previously, the CCL5/CCR5 interaction was shown to upregulate the cytotoxic function and proliferation of TCR-stimulated

(C) Sorted memory CD45.1$^+$OT-1 T cells (n = 7) were cultured with or without IL-15/IL-15R (20 ng/mL) for 48 h. The percentages of CCR5$^+$, CCR2$^+$, and CXCR3$^+$ cells among CD45.1$^+$OT-1 T cells were analyzed. Representative FACS plots (upper) and summary data (left) are presented.
(D) Sorted memory CD45.1$^+$OT-1 T cells (n = 7) were stimulated with IL-15/IL-15R (20 ng/mL), SIINFEKL peptide (1 μg/mL), or both for 48 h. The percentages of CCR5$^+$ among CD45.1$^+$OT-1 T cells were analyzed. Summary data are presented.
(E and F) Memory CD45.1$^+$OT-1 T cells were treated with mock (n = 7), IL-15/IL-15R (20 ng/mL; n = 7), or IL-15/IL-15R with Maraviroc (10 μM; n = 7) for 48 h and adoptively transferred to C57BL/6 mice. Recipient mice were infected intranasally with the PR8 strain of influenza A virus (200 pfu). (E) Absolute count of CD45.1$^+$OT-1 T cells migrating to the lungs of recipient mice on post-infection day 2 as analyzed by flow cytometry. Representative FACS plots (left) and summary data (right) are presented. (F) Frequency of Ki-67$^+$ cells among CD45.1$^+$OT-1 T cells migrating to the lung of recipient mice was analyzed by flow cytometry. A representative FACS plot (left) and summary data (right) are presented.
Data are presented as mean and SD. Statistical analysis was performed using the Wilcoxon signed-rank test (B–D) or Mann-Whitney U test (E and F). N.S., not significant; *p < 0.05, **p < 0.01, ***p < 0.001.

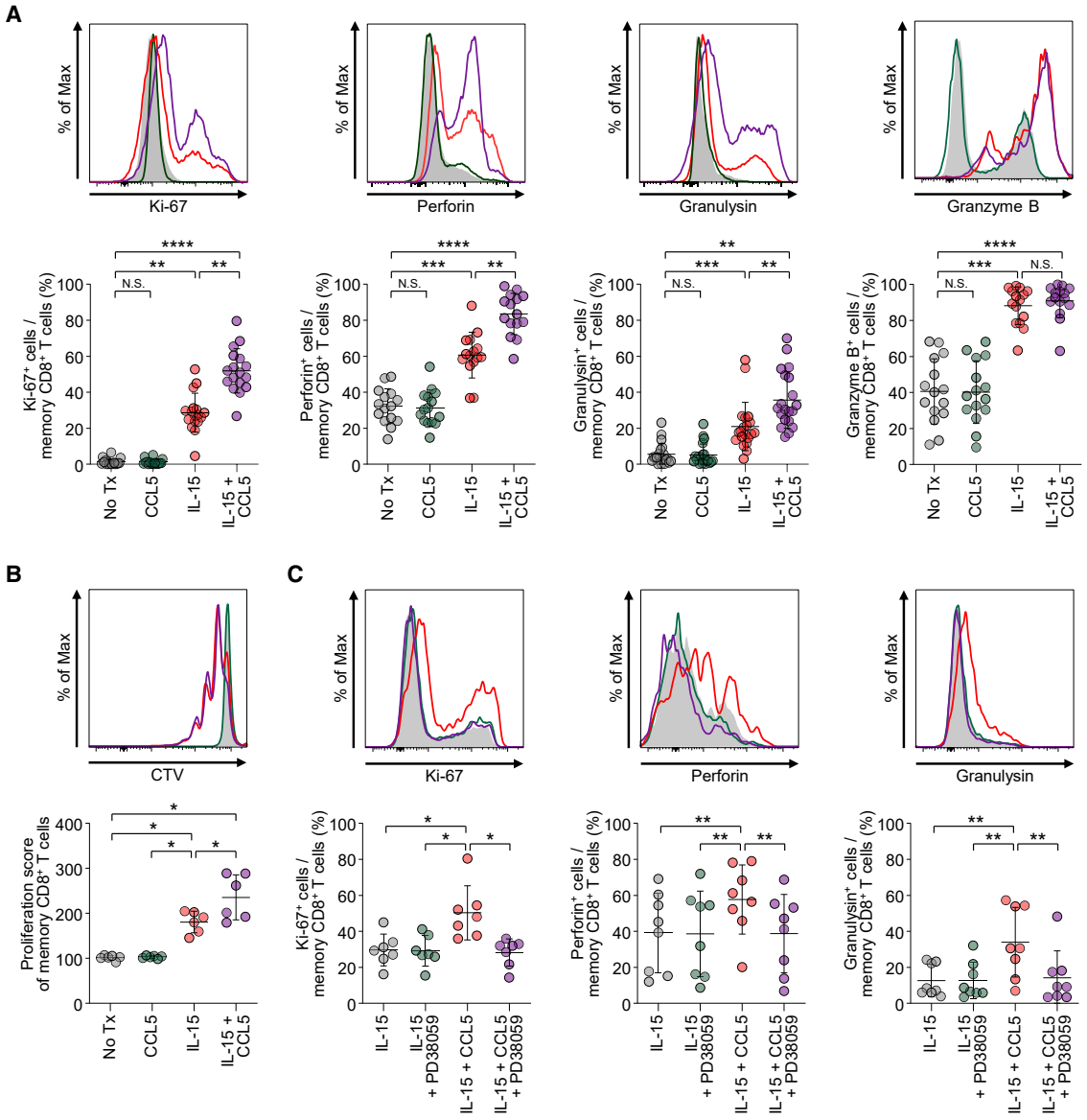

Figure 3. CCL5/CCR5 interaction enhanced proliferation and expression of cytotoxic molecules in IL-15-stimulated CCR7$^-$CD8$^+$ T cells

(A and B) CellTrace Violet (CTV)-labeled (B) or unlabeled (A) PBMCs from healthy donors were stimulated with CCL5 (100 ng/mL), IL-15 (10 ng/mL), or both and analyzed by flow cytometry. (A) Frequency of Ki-67$^+$ (n = 17), perforin$^+$ (n = 15), granulysin$^+$ (n = 20), and granzyme B$^+$ (n = 15) cells was analyzed in gated CCR7$^-$CD8$^+$ T cells. Representative FACS plots (upper) and summary data (lower) are presented. (B) Proliferation score for CCR7$^-$CD8$^+$ T cells (n = 6) was analyzed by CTV dilution, and representative FACS plots (upper) and summary data (lower) are presented.

(C) PBMCs from healthy donors were stimulated with IL-15 (10 ng/mL) for 48 h and further cultured with ERK inhibitor (PD98059), CCL5, or both for 24 h. The frequency of Ki-67$^+$ (n = 7), perforin$^+$ (n = 8), and granulysin$^+$ (n = 8) cells was examined among gated CCR7$^-$CD8$^+$ T cells, and representative FACS plots (upper) and summary data (lower) are presented.

Data are presented as mean and SD. N.S., not significant; *p < 0.05, **p < 0.01, ***p < 0.001, ****p < 0.0001; Wilcoxon matched-pairs signed-rank test.

T cells (Taub et al., 1996). These data support our current results, although the previous studies stimulated total CD3$^+$ T cells with CCL5 in combination with anti-CD3, not IL-15. The CCL5/CCR5 interaction plays a role not only in recruiting IL-15-induced bystander-activated CD8$^+$ T cells, but also in enhancing their proliferation and cytotoxic capacity.

The role of CCR5 in bystander-activated CD8$^+$ T cells may be important in human diseases in which IL-15 is over-produced. We previously showed that IL-15-induced bystander-activated CD8$^+$ T cells are associated with liver immunopathology in patients with AHA (Kim et al., 2018). In the current study, the expression of CCR5 increased in HAV-unrelated, CMV-specific memory CD8$^+$ T cells from patients with AHA compared with HAV-specific CD8$^+$ T cells, although we examined single CD8$^+$ T cell specificity for each virus. In addition, more CCR5$^+$ cells were present among liver-infiltrating CD8$^+$ T cells than among

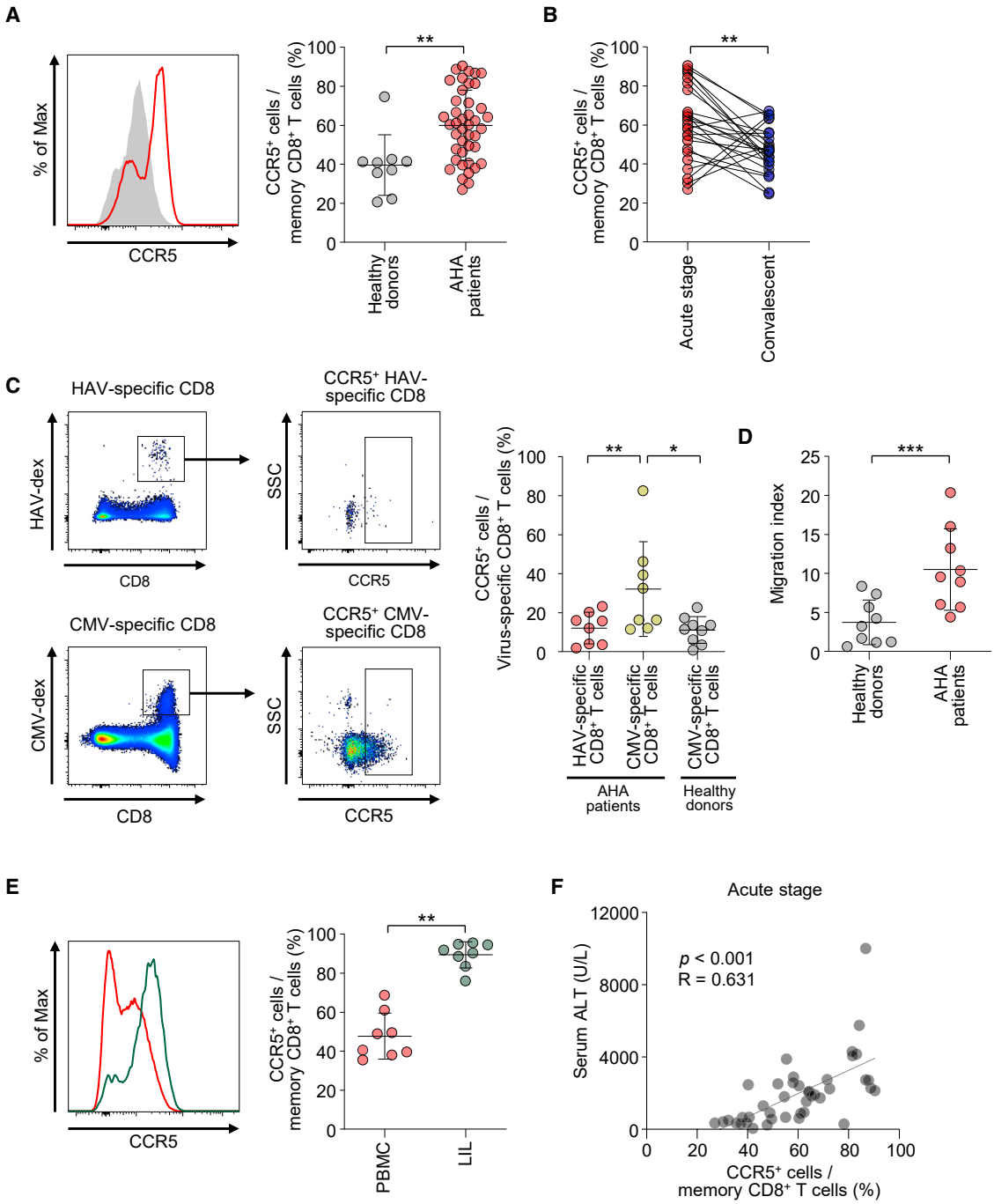

Figure 4. CCR5 upregulation on HAV-unrelated virus-specific CD8⁺ T cells during AHA

PBMCs from healthy donors and patients with AHA were analyzed by flow cytometry.

(A) Frequency of CCR5⁺ cells among CCR7⁻CD8⁺ T cells was analyzed in healthy donors (n = 9) and patients with AHA (n = 42). A representative FACS plot (left) and summary data (right) are presented.

(B) Frequency of CCR5⁺ cells among CCR7⁻CD8⁺ T cells was analyzed in patients with AHA (n = 25) in the acute stage and convalescent stage.

(C) Frequency of CCR5⁺ cells was analyzed among HLA-A*0201 HAV $3D_{2026}$ (LLYNCCYHV) multimer⁺ and HLA-A*0201 CMV $pp65_{495}$ (NLVPMVATV) multimer⁺CD8⁺ T cells from patients with AHA (n = 8) and among CMV $pp65_{495}$ (NLVPMVATV) multimer⁺CD8⁺ T cells from healthy donors (n = 9).

(D) Migration index of CCR7⁻CD8⁺ T cells from healthy donors (n = 9) and patients with AHA (n = 9) was analyzed in transwell migration assays.

(E) Frequency of CCR5⁺ cells among CCR7⁻CD8⁺ T cells was analyzed in paired PBMCs and liver-infiltrating lymphocytes from patients with AHA (n = 8).

(F) Frequency of CCR5⁺ cells among CCR7⁻CD8⁺ T cells was analyzed for a correlation with serum ALT levels in the acute stage of AHA (n = 42).

Data are presented as mean and SD. Statistical analysis was performed using the Mann-Whitney U test (A, C, and D), Wilcoxon matched-pairs signed-rank test (B and E), or Pearson's correlation test (F). *p < 0.05, **p < 0.01, ***p < 0.001.

peripheral blood CD8$^+$ T cells. We previously showed that CCL5 is produced by HAV-infected cells in a type III interferon-dependent manner and that CCL5 levels are increased in patients with AHA (Sung et al., 2017). Altogether, these data indicate that the CCL5-CCR5 signals play an important role in the migration of IL-15-induced bystander-activated CD8$^+$ T cells to HAV-infected livers. For the homing of HAV-specific CD8$^+$ T cells, we hypothesized that other chemokine receptors, such as CXCR3, play a major role, although we did not examine this point in the current study. Our group previously demonstrated that HAV infection strongly increases the production of not only CCR5 ligands but also a CXCR3 ligand, CXCL10 (Sung et al., 2017). Finally, we found that the expression of CCR5 in CD8$^+$ T cells significantly correlates with serum ALT levels among patients with AHA. However, we could not conclude that recruited CCR5$^+$CD8$^+$ T cells cause the liver injury, because there is a chance that the recruitment of CCR5$^+$CD8$^+$ T cells results from severe inflammation and liver injury.

In summary, our data demonstrate that the migration of bystander-activated CD8$^+$ T cells is mediated by IL-15-induced CCR5 and that the CCL5/CCR5 interaction enhances the proliferation and cytotoxic capacity of IL-15-induced bystander-activated CD8$^+$ T cells. Our current study provides an understanding of how bystander-activated CD8$^+$ T cells migrate to sites of inflammation and contribute to immunopathology during acute viral infection.

STAR★METHODS

Detailed methods are provided in the online version of this paper and include the following:

- KEY RESOURCES TABLE
- RESOURCE AVAILABILITY
  - Lead contact
  - Materials availability
  - Data and code availability
- EXPERIMENTAL MODEL AND SUBJECT DETAILS
  - Patients and specimens
  - Mice
- METHOD DETAILS
  - Flow cytometry
  - RNA sequencing and data analysis
  - *In vitro* cytokine stimulation
  - Transwell migration assay
  - *In vivo* migration study
  - *In vitro* chemokine stimulation
- QUANTIFICATION AND STATISTICAL ANALYSIS

SUPPLEMENTAL INFORMATION

Supplemental information can be found online at https://doi.org/10.1016/j.celrep.2021.109438.

ACKNOWLEDGMENTS

This work was supported by the Samsung Science and Technology Foundation under project SSTF-BA1402-51. The graphical abstract was created with Biorender.com.

AUTHOR CONTRIBUTIONS

I.-H.S., S.-H.P., and E.-C.S. designed the experiments and managed the study. I.-H.S., H.S.E., J.K.K., H.L., S.J., S.J.C., and J.L. performed the experiments. I.-H.S., H.S.E., and J.K.K. analyzed the data. B.S.L., S.H.K., W.S.R., D.H.L., and W.K. provided human clinical samples I.-H.S., S.-H.P., and E.-C.S. conceived the work and wrote the manuscript, which was revised and approved by all authors.

DECLARATION OF INTERESTS

The authors declare no competing interests.

Received: October 8, 2020
Revised: April 17, 2021
Accepted: July 2, 2021
Published: July 27, 2021

REFERENCES

Alanio, C., Nicoli, F., Sultanik, P., Flecken, T., Perot, B., Duffy, D., Bianchi, E., Lim, A., Clave, E., van Buuren, M.M., et al. (2015). Bystander hyperactivation of preimmune CD8+ T cells in chronic HCV patients. eLife *4*, e07916.

Bastidas, S., Graw, F., Smith, M.Z., Kuster, H., Günthard, H.F., and Oxenius, A. (2014). CD8+ T cells are activated in an antigen-independent manner in HIV-infected individuals. J. Immunol. *192*, 1732–1744.

Chu, T., Tyznik, A.J., Roepke, S., Berkley, A.M., Woodward-Davis, A., Pattacini, L., Bevan, M.J., Zehn, D., and Prlic, M. (2013). Bystander-activated memory CD8 T cells control early pathogen load in an innate-like, NKG2D-dependent manner. Cell Rep. *3*, 701–708.

Crosby, E.J., Goldschmidt, M.H., Wherry, E.J., and Scott, P. (2014). Engagement of NKG2D on bystander memory CD8 T cells promotes increased immunopathology following *Leishmania* major infection. PLoS Pathog. *10*, e1003970.

Doisne, J.M., Urrutia, A., Lacabaratz-Porret, C., Goujard, C., Meyer, L., Chaix, M.L., Sinet, M., and Venet, A. (2004). CD8+ T cells specific for EBV, cytomegalovirus, and influenza virus are activated during primary HIV infection. J. Immunol. *173*, 2410–2418.

Judge, A.D., Zhang, X., Fujii, H., Surh, C.D., and Sprent, J. (2002). Interleukin 15 controls both proliferation and survival of a subset of memory-phenotype CD8(+) T cells. J. Exp. Med. *196*, 935–946.

Kim, T.S., and Shin, E.C. (2019). The activation of bystander CD8$^+$ T cells and their roles in viral infection. Exp. Mol. Med. *51*, 1–9.

Kim, J., Chang, D.Y., Lee, H.W., Lee, H., Kim, J.H., Sung, P.S., Kim, K.H., Hong, S.H., Kang, W., Lee, J., et al. (2018). Innate-like Cytotoxic Function of Bystander-Activated CD8$^+$ T Cells Is Associated with Liver Injury in Acute Hepatitis A. Immunity *48*, 161–173.e5.

Kim, J.H., Han, J.W., Choi, Y.J., Rha, M.S., Koh, J.Y., Kim, K.H., Kim, C.G., Lee, Y.J., Kim, A.R., Park, J., et al. (2020). Functions of human liver CD69$^+$CD103$^-$CD8$^+$ T cells depend on HIF-2α activity in healthy and pathologic livers. J. Hepatol. *72*, 1170–1181.

Liu, K., Catalfamo, M., Li, Y., Henkart, P.A., and Weng, N.P. (2002). IL-15 mimics T cell receptor crosslinking in the induction of cellular proliferation, gene expression, and cytotoxicity in CD8$^+$ memory T cells. Proc. Natl. Acad. Sci. USA *99*, 6192–6197.

Lu, J., Giuntoli, R.L., 2nd, Omiya, R., Kobayashi, H., Kennedy, R., and Celis, E. (2002). Interleukin 15 promotes antigen-independent *in vitro* expansion and long-term survival of antitumor cytotoxic T lymphocytes. Clin. Cancer Res. *8*, 3877–3884.

Maurice, N.J., McElrath, M.J., Andersen-Nissen, E., Frahm, N., and Prlic, M. (2019). CXCR3 enables recruitment and site-specific bystander activation of memory CD8$^+$ T cells. Nat. Commun. *10*, 4987.

Perera, L.P., Goldman, C.K., and Waldmann, T.A. (1999). IL-15 induces the expression of chemokines and their receptors in T lymphocytes. J. Immunol. *162*, 2606–2612.

Rha, M.S., Han, J.W., Kim, J.H., Koh, J.Y., Park, H.J., Kim, S.I., Kim, M.S., Lee, J.G., Lee, H.W., Lee, D.H., et al. (2020). Human liver $CD8^+$ MAIT cells exert TCR/MR1-independent innate-like cytotoxicity in response to IL-15. J. Hepatol. *73*, 640–650.

Sandalova, E., Laccabue, D., Boni, C., Tan, A.T., Fink, K., Ooi, E.E., Chua, R., Shafaeddin Schreve, B., Ferrari, C., and Bertoletti, A. (2010). Contribution of herpesvirus specific CD8 T cells to anti-viral T cell response in humans. PLoS Pathog. *6*, e1001051.

Soudja, S.M., Ruiz, A.L., Marie, J.C., and Lauvau, G. (2012). Inflammatory monocytes activate memory CD8(+) T and innate NK lymphocytes independent of cognate antigen during microbial pathogen invasion. Immunity *37*, 549–562.

Sung, P.S., Hong, S.H., Lee, J., Park, S.H., Yoon, S.K., Chung, W.J., and Shin, E.C. (2017). CXCL10 is produced in hepatitis A virus-infected cells in an IRF3-dependent but IFN-independent manner. Sci. Rep. *7*, 6387.

Taub, D.D., Ortaldo, J.R., Turcovski-Corrales, S.M., Key, M.L., Longo, D.L., and Murphy, W.J. (1996). Beta chemokines costimulate lymphocyte cytolysis, proliferation, and lymphokine production. J. Leukoc. Biol. *59*, 81–89.

Tough, D.F., Borrow, P., and Sprent, J. (1996). Induction of bystander T cell proliferation by viruses and type I interferon *in vivo*. Science *272*, 1947–1950.

Tuuminen, T., Kekäläinen, E., Mäkelä, S., Ala-Houhala, I., Ennis, F.A., Hedman, K., Mustonen, J., Vaheri, A., and Arstila, T.P. (2007). Human CD8+ T cell memory generation in Puumala hantavirus infection occurs after the acute phase and is associated with boosting of EBV-specific CD8+ memory T cells. J. Immunol. *179*, 1988–1995.

Whiteside, S.K., Snook, J.P., Williams, M.A., and Weis, J.J. (2018). Bystander T Cells: A Balancing Act of Friends and Foes. Trends Immunol. *39*, 1021–1035.

Wong, P., and Pamer, E.G. (2003). CD8 T cell responses to infectious pathogens. Annu. Rev. Immunol. *21*, 29–70.

Younes, S.A., Freeman, M.L., Mudd, J.C., Shive, C.L., Reynaldi, A., Panigrahi, S., Estes, J.D., Deleage, C., Lucero, C., Anderson, J., et al. (2016). IL-15 promotes activation and expansion of CD8+ T cells in HIV-1 infection. J. Clin. Invest. *126*, 2745–2756.

STAR★METHODS

KEY RESOURCES TABLE

REAGENT or RESOURCE	SOURCE	IDENTIFIER
Antibodies		
BV711 Anti-mouse CD192 (CCR2) (475301)	BD Biosciences	Cat# 747964; RRID: AB_2872425
BV421 Anti-human CD195 (CCR5) (2D7/CCR5)	BD Biosciences	Cat# 562576; RRID: AB_2737661
BV421 Anti-mouse CD195 (CCR5) (C34-3448)	BD Biosciences	Cat# 743695; RRID: AB_2741677
BB700 Anti-human CD127 (HIL-7R-M21)	BD Biosciences	Cat# 566398; RRID: AB_2744279
BV786 Anti-human CD127 (HIL-7R-M21)	BD Biosciences	Cat# 563324; RRID: AB_2738138
BV786 Anti-human CD25 (M-A251)	BD Biosciences	Cat# 563701; RRID: AB_2744338
BB515 Anti-human CD25 (2A3)	BD Biosciences	Cat# 564467; RRID: AB_2744340
Alexa Fluor 700 Anti-human CD3 (UCHT1)	BD Biosciences	Cat# 557943; RRID: AB_396952
BV786 Anti-mouse CD3e (145-2C11)	BD Biosciences	Cat# 564379; RRID: AB_2738780
PerCP-Cy 5.5 Anti-human CD4 (RPA-T4)	BD Biosciences	Cat# 560650; RRID: AB_1727476
BV605 Anti-mouse CD44 (IM7)	BD Biosciences	Cat# 563058; RRID: AB_2737979
Alexa Fluor 700 Anti-mouse CD45.1 (A20)	BD Biosciences	Cat# 561235; RRID: AB_10611577
APC-H7 Anti-human CD45RA (HI100)	BD Biosciences	Cat# 560674; RRID: AB_1727497
BV650 Anti-human CD8 (RPA-T8)	BD Biosciences	Cat# 563821; RRID: AB_2744462
BV711 Anti-human CD8 (RPA-T8)	BD Biosciences	Cat# 563677; RRID: AB_2744463
APC Anti-mouse CD8a (53-6.7)	BD Biosciences	Cat# 560182; RRID: AB_1645237
PE Anti-human CX3CR1 (2A9-1)	BD Biosciences	Cat# 565796; RRID: AB_2739360
BB700 Anti-mouse CD183 (CXCR3) (CXCR3-173)	BD Biosciences	Cat# 742274; RRID: AB_2871450
Alexa Fluor 647 Anti-human Granzyme B (GB11)	BD Biosciences	Cat# 560212; RRID: AB_11154033
BV421 Anti-human IgG2a, k Isotype Control (G155-178)	BD Biosciences	Cat# 562439; RRID: AB_11151914
PE Anti-human CD314 (NKG2D) (1D11)	BD Biosciences	Cat# 557940; RRID: AB_396951
PE Anti-human CD192 (CCR2) (K036C2)	BioLegend	Cat# 357206; RRID: AB_2562059
PerCP-Cy 5.5 Anti-human CD197 (CCR7) (G043H7)	BioLegend	Cat# 353220; RRID: AB_10916121
FITC Anti-human CD28 (CD28.2)	BioLegend	Cat# 302906; RRID: AB_314308
BV650 Anti-human CX3CR1 (2A9-1)	BioLegend	Cat# 341626; RRID: AB_2716245
APC Anti-human CD183 (CXCR3) (G025H7)	BioLegend	Cat# 353708; RRID: AB_10983064
PE Anti-human Ki-67 (Ki-67)	BioLegend	Cat# 350504; RRID: AB_10660752
APC Anti-mouse CD314 (NKG2D) (CX5)	BioLegend	Cat# 130212; RRID: AB_1236372
BV421 Anti-human Perforin (dG9)	BioLegend	Cat# 308122; RRID: AB_2566204
PE-eFluor 610 Anti-human CD4 (RPA-T4)	eBioscience	Cat# 61-0049-42; RRID: AB_2574522
PE-Cy7 Anti-human CD57 (TB01)	eBioscience	Cat# 25-0577-42; RRID: AB_2573354
PE Anti-human Granulysin (eBioDH2)	eBioscience	Cat# 12-8828-42; RRID: AB_10854120
FITC Anti-mouse Ki-67 (SolA15)	eBioscience	Cat# 11-5698-82; RRID: AB_11151330
PE Anti-mouse Nur77 (12.14)	eBioscience	Cat# 12-5965-82; RRID: AB_1257209
PE Anti-human FOXP3 (PCH101)	Invitrogen	Cat# 12-4776-42; RRID: AB_1518782
CD3 pure-functional grade, human (OKT3)	Miltenyi Biotec	Cat# 130-093-387; RRID: AB_1036144
PE Anti-mouse CD45.1 (A20)	Miltenyi Biotec	Cat# 130-102-499; RRID: AB_2660704
Fluorescein-conjugated Anti-human CCR7 (150503)	R&D Systems	Cat# FAB197F; RRID: AB_2259847

(*Continued on next page*)

Continued

REAGENT or RESOURCE	SOURCE	IDENTIFIER
Bacterial and virus strains		
A/Puerto Rico/8/1934 (PR8)		N/A
Chemicals, peptides, and recombinant proteins		
Recombinant Human CCL3 (MIP-1a) (carrier-free)	BioLegend	Cat# 759504
Recombinant Human CCL4 (MIP-1b) (carrier-free)	BioLegend	Cat# 554704
Recombinant Human CCL5 (RANTES) (carrier-free)	BioLegend	Cat# 580204
Recombinant human IL-15 protein	Peprotech	Cat# 200-15
Recombinant human IL-7 protein	Peprotech	Cat# 200-07
Recombinant human IL-2 protein	R&D Systems	Cat# 202-IL-010
CMV peptide NLVPMVATV	Peptron	Customized
SIINFEKL peptide	Peptron	Customized
Critical commercial assays		
6.5mm Transwell with 5.0 μm Pore Polycarbonate Membrane Insert	Corning	Cat# 3421
Foxp3/TF staining Buffer Set Kit	eBioscience	Cat# 00-5523-00
CellTrace Violet Cell Proliferation Kit	Invitrogen	Cat# C34557
CountBright Absolute Counting Beads	Invitrogen	Cat# C36950
LIVE/DEAD Fixable Aqua Dead Cell Stain Kit	Invitrogen	Cat# L34966
LIVE/DEAD Fixable Red Dead Cell Stain Kit	Invitrogen	Cat# L23102
TRIzol LS Reagent	Invitrogen	Cat# 10296028
Anti-PE MicroBeads	Miltenyi biotec	Cat# 130-048-801
CD197 (CCR7)-Biotin, human	Miltenyi biotec	Cat# 130-108-282
CD197 (CCR7)-Biotin, human	Miltenyi biotec	Cat# 130-120-467
CD8+ T Cell Isolation Kit, human	Miltenyi biotec	Cat# 130-096-495
Maraviroc	TOCRIS	Cat# 3756-10
PD98059	TOCRIS	Cat# 1213
Deposited data		
RNA-seq, *H. sapiens*	This manuscript	SRR14699626; https://www.ncbi.nlm.nih.gov/sra
RNA-seq, *H. sapiens*	This manuscript	SRR14699627; https://www.ncbi.nlm.nih.gov/sra
RNA-seq, *H. sapiens*	This manuscript	SRR14699628; https://www.ncbi.nlm.nih.gov/sra
RNA-seq, *H. sapiens*	This manuscript	SRR14699629; https://www.ncbi.nlm.nih.gov/sra
RNA-seq, *H. sapiens*	This manuscript	SRR14699630; https://www.ncbi.nlm.nih.gov/sra
RNA-seq, *H. sapiens*	This manuscript	SRR14699631; https://www.ncbi.nlm.nih.gov/sra
RNA-seq, *H. sapiens*	This manuscript	SRR14699632; https://www.ncbi.nlm.nih.gov/sra
RNA-seq, *H. sapiens*	This manuscript	SRR14699633; https://www.ncbi.nlm.nih.gov/sra
Experimental models: Organisms/strains		
Mouse: C57BL/6 (B6)	The Jackson Laboratory	N/A
Mouse: OT-1	In House	N/A

(*Continued on next page*)

Continued

REAGENT or RESOURCE	SOURCE	IDENTIFIER
Software and algorithms		
FlowJo (version 10.7)	Tree Star	https://www.flowjo.com/solutions/flowjo/downloads
Prism (version 6)	GraphPad	N/A
Other		
NLVPMVATV (pp65495) HLA-A*0201 Dextramer	Immudex	Cat# WB2132-APC
LLYNCCYHV (HAV 3D2026) HLA-A*0201 Dextramer	Immudex	Cat# WB5515-APC

RESOURCE AVAILABILITY

Lead contact

Further information and requests for resources and reagents should be directed to and will be fulfilled by the Lead Contact, Eui-Cheol Shin (ecshin@kaist.ac.kr).

Materials availability

This study did not generate new unique reagents.

Data and code availability

RNA-seq data have been deposited at SRA and are publicly available as of the date of publication. Accession numbers are listed in the Key Resources Table. All original code in this paper will be shared by the lead contact upon request. Any additional information required to reanalyze the data reported in this paper is available from the lead contact upon request.

EXPERIMENTAL MODEL AND SUBJECT DETAILS

Patients and specimens

This study included 42 patients (male, 30; female, 12; age, median, 37; age, range, 20-50) diagnosed with AHA and hospitalized in SMG-SNU Boramae Medical Center (Seoul, Republic of Korea) and Chungnam National University Hospital (Daejeon, Republic of Korea). All patients were seropositive for both anti-HAV IgM and IgG and had clinical and laboratory features of acute hepatitis. Whole blood and serum were collected; PBMCs were isolated by Ficoll (GE Healthcare) density-gradient centrifugation and cryopreserved. Fresh liver tissue was obtained from eight patients at SMG-SNU Boramae Medical Center (male, 5; female, 3; age, median, 35.5; age, range, 20-46). Information on the 42 patients with AHA is provided in Table S1. This study was conducted according to the principles of the Declaration of Helsinki and approved by the institutional review boards of each institution where samples were obtained (SMG-SNU Boramae Medical Center and Chungnam National University Hospital). Written informed consent was obtained from each patient prior to inclusion in the study.

Mice

Six-week-old female C57BL/6 mice were purchased from Jackson Laboratory and housed at Korea Advanced Institute of Science and Technology (KAIST) under SPF conditions. All experiments followed the protocols approved by the KAIST Institutional Animal Care and Use Committee.

METHOD DETAILS

Flow cytometry

Cryopreserved PBMCs were thawed and stained with fluorochrome-conjugated antibodies for 30 min at 4°C. Following cell surface staining, cells were permeabilized and intracellular staining buffer (eBioscience) used to stain intracellular markers, such as FOXP3, granzymes, perforin, granulysin, and Ki-67. Cells were also stained with an HLA multimer for 15 min at room temperature. In this study, we used the following MHC class I multimers to detect CMV- and HAV-specific $CD8^+$ T cells: HLA-A*0201 CMV $pp65_{495}$ (NLVPMVATV) and HLA-A*0201 HAV $3D_{2026}$ (LLYNCCYHV). Multicolor flow cytometry was performed using an LSR II instrument (BD Biosciences) and data analyzed using FlowJo software (Treestar).

RNA sequencing and data analysis

RNA sequencing (RNA-seq) was performed on sorted $CCR7^-CD8^+$ T cells treated with IL-15 (n = 4) or PBS (n = 4). Total RNA quality was assessed by the Agilent 2100 Bioanalyzer System. Extracted RNA samples were processed using the QuantSeq 3′ mRNA-Seq

Library Prep Kit (Lexogen) and sequenced on an Illumina NextSeq 500. A median 2.0 × 10^7 (range, 1.7 × 10^7 to 2.4 × 10^7) single-end reads with 76 base pairs were generated. Reads were trimmed based on sequencing quality using Sickle (GitHub, San Francisco, CA). Trimmed reads were aligned on a human reference sequence (hg19) using Tophat. The number of mapped reads on the 3′ end of each gene was calculated using Bedtools. Gene counts were normalized by library size and the differential expression of genes analyzed using DESeq2 (v.1.24.0). Raw files are accessible under the Sequence Read Archive accession number SRR14699626, SRR14699627, SRR14699628, SRR14699629, SRR14699630, SRR14699631, SRR14699632, and SRR14699633.

In vitro cytokine stimulation

PBMCs from healthy donors were cultured in the presence of IL-2 (10 ng/mL; R&D Systems), IL-7 (10 ng/mL; Peprotech), IL-15 (10 ng/mL; Peprotech), anti-CD3 (1 μg/mL; Miltenyi biotec), or IL-15 with anti-CD3 for 48 h and examined for the expression of chemokine receptors, including CCR2, CCR5, CXCR3, and CX3CR1, in gated $CCR7^-CD8^+$ T cells or HLA multimer$^+CCR7^-CD8^+$ T cells. PBMCs from healthy donors were cultured in the presence of IL-15 (10 ng/mL; Peprotech), CMV $pp65_{495}$ peptide (NLVPMVATV) (1 μg/mL; Peptron), or both for 48 h and analyzed for the expression of CCR5 in gated $CCR7^-CD8^+$ T cells. For the detection of CCR5 expression in $CCR7^-CD8^+$ T cells, PBMCs and sorted $CCR7^-CD8^+$ T cells from healthy donors were cultured in the presence of IL-15 (10 ng/mL; Peprotech) for 48 h and examined for the expression of CCR5 in gated $CCR7^-CD8^+$ T cells. In preliminary experiments, we had found that the frequency of $CCR5^+$ cells increased with IL-15 treatment for up to 48 hours, and then was maintained thereafter. Therefore, we chose 48 hours as the culture period.

Transwell migration assay

Sorted $CCR7^-CD8^+$ T cells from healthy donors were treated with IL-15 or PBS for 48 h. Each group of $CCR7^-CD8^+$ T cells was seeded in the upper well with a permeable membrane, and media containing PBS or CCL5 was placed in the lower well. Following an incubation period of 3 h, the cells that migrated through the membrane were stained and counted using CountBright Absolute Counting Beads.

In vivo migration study

$CD45.1^+$OT-1 $CD8^+$ T cells (1 ~3 × 10^5 cells) were adoptively transferred into B6 mice and primed by VV-OVA infection. After resolution of VV-OVA infection, memory OT-1 $CD8^+$ T cells were sorted from the spleens using the CD45.1 congenic marker and cultured in the presence of mouse IL-15/IL-15R complex recombinant protein (20 ng/mL; eBioscience) or PBS for 48 h and examined for the expression of CCR2, CXCR3, and CCR5. These IL-15/IL-15R stimulated cells (6x10^5 cells in 100 μL PBS, 48 h) or unstimulated $CD45.1^+$OT-1 T cells (6x10^5 cells in 100 μL PBS) were injected into the tail veins of the recipient mice (C57BL/6). After 8 h, the recipient mice were infected with PR8 influenza A virus (intranasal; 200 PFU). After 48 h of influenza infection, the lungs of recipient mice were harvested and analyzed by flow cytometry (LSR II; BD Biosciences). Sorted memory $CD45.1^+$OT-1 T cells were cultured in the presence of mouse IL-15/IL-15R complex recombinant protein (20 ng/mL; eBioscience), SIINFEKL peptide (1 μg/mL; Peptron) or both for 48 h and examined for the expression of CCR5.

In vitro chemokine stimulation

PBMCs pre-stimulated with IL-15 for 48 h were cultured in the presence of CCL3, CCL4, and CCL5 for an additional 24 h and examined for the expression of Ki-67, perforin, granulysin, and granzyme B in gated $CCR7^-CD8^+$ T cells. To assess cellular proliferation, we stained cells using CellTrace Violet cell proliferation kit (Thermo Fisher Scientific) according to the manufacturer's instructions. A proliferation score was calculated by averaging the number of divisions in $CCR7^-CD8^+$ T cells. To investigate the contribution of ERK signaling to the CCL5/CCR5 interaction in IL-15-stimulated memory $CD8^+$ T cells, the cells were treated with ERK inhibitor (PD98059) for 30 min before chemokine treatment.

QUANTIFICATION AND STATISTICAL ANALYSIS

Statistical analyses were performed in Prism 7 (GraphPad Software, San Diego, CA, USA). All data are presented as the mean ± standard deviation. We used the Mann-Whitney U-test to compare two groups in each experiment. Correlation studies were performed by Spearman's rank correlation analysis. All of the statistical details of experiments can be found in the figure legends.